

# Effects of Additive Amount on Microstructure and Fracture Toughness of SiC–TiB<sub>2</sub> Composites

Kyeong-Sik Cho,\* Heon-Jin Choi & June-Gunn Lee

Division of Ceramics, Korea Institute of Science and Technology, PO Box 131, Cheongryang, Seoul 130-650, Korea

Young-Wook Kim

Department of Materials Science and Engineering, Seoul City University, 90 Jeonnong-Dong, Dongdaemoon-Ku, Seoul 130-743, Korea

(Received 10 October 1996; accepted 11 December 1996)

**Abstract:** Powder mixtures of  $\beta$ -SiC–30 wt% TiB<sub>2</sub> containing 5 wt% (ST1), 10 wt% (ST2), and 20 wt% (ST3) Al<sub>2</sub>O<sub>3</sub>–Y<sub>2</sub>O<sub>3</sub> as sintering additives were liquid-phase sintered at 1850°C for 1 h by hot-pressing and subsequently annealed at 1950°C for 2, 6, and 12 h. These materials had a microstructure of ‘in situ-toughened composites’ as a result of the  $\beta \rightarrow \alpha$  phase transformation of SiC during annealing. The introduction of larger amount of additives accelerated the grain growth of elongated  $\alpha$ -SiC grains with higher aspect ratio, resulting in the improved fracture toughness. The fracture toughnesses of 12-h annealed materials with 5, 10, and 20 wt% additives were 5.7, 5.9, and 7.1 MPa m<sup>1/2</sup>, respectively.  
© 1998 Elsevier Science Limited and Techna S.r.l. All rights reserved

## 1 INTRODUCTION

Densification of SiC–TiB<sub>2</sub> composites without the aids of high pressure or sintering additives is very difficult owing to the covalent nature of their bonds. Therefore, sintering additives such as metals, oxides, and non-oxides are usually added to densify the composites. Composites of SiC–TiB<sub>2</sub> can be fabricated by hot-pressing with the aid of C and Al or B<sup>1,2</sup> or pressureless sintering with in-situ synthesis of TiB<sub>2</sub> through a reaction between TiB<sub>2</sub> and B<sup>3</sup> to a near full density at temperatures in excess of 2000°C. The role of additives for the sintering of covalent-bonded ceramics can be regarded as not only densification aids but also key elements for the microstructural development, since the related properties of materials are influenced by the kinds and amounts of additives.<sup>4–6</sup> Several investigations have shown that the dispersion of TiB<sub>2</sub> particles results in improved fracture toughness of SiC ceramics.<sup>3,7,8</sup> It is claimed that the residual stresses due to the thermal expansion

mismatch between TiB<sub>2</sub> ( $8.6 \times 10^{-6} \text{ } ^\circ\text{C}^{-1}$ ) and SiC ( $4.2 \times 10^{-6} \text{ } ^\circ\text{C}^{-1}$ ) improve toughness by deflecting the cracks around the TiB<sub>2</sub> particles.<sup>2,3</sup>

Recently, liquid-phase sintering of SiC–TiB<sub>2</sub> composites at a temperature as low as 1850°C<sup>9</sup> and a new in-situ processing strategy based on liquid phase sintering and subsequent annealing for tailoring SiC–TiB<sub>2</sub> composites<sup>10</sup> have been reported. Using Y<sub>2</sub>O<sub>3</sub> and Al<sub>2</sub>O<sub>3</sub> as sintering additives, a unique microstructure consisting of uniformly distributed, elongated  $\alpha$ -SiC grains, equiaxed TiB<sub>2</sub> grains, and yttrium aluminium garnet (Y<sub>3</sub>Al<sub>5</sub>O<sub>12</sub>, YAG) as a grain boundary phase was obtained. The fracture toughness of the SiC–30 wt% TiB<sub>2</sub> composites after 6 h annealing at 1950°C was 6.7 MPa m<sup>1/2</sup>, approximately 50% higher than that (4.4 MPa m<sup>1/2</sup>) of as-hot-pressed composites. The presence of elongated  $\alpha$ -SiC grains and weak interface boundaries have been identified as the principal elements of effective grain bridging and deflection, resulting in increased fracture toughness.<sup>10,11</sup>

In this study, we present the influence of additive amount on microstructure and fracture toughness of SiC–30 wt% TiB<sub>2</sub> composites with Al<sub>2</sub>O<sub>3</sub>–Y<sub>2</sub>O<sub>3</sub>

\*To whom correspondence should be addressed.

**Table 1. Characteristics of SiC–30 wt% TiB<sub>2</sub> composites**

Materials	Composition (wt%)				Annealing time at 1950°C (h)	Relative density (%)	XRD derived crystalline phase	
	SiC	TiB <sub>2</sub>	Al <sub>2</sub> O <sub>3</sub>	Y <sub>2</sub> O <sub>3</sub>			Major	Trace
ST1	65	30	3.5	1.5	0	97.3	β-SiC, TiB <sub>2</sub>	
					2	97.0	β-SiC, TiB <sub>2</sub>	α-SiC
					6	96.9	α-SiC, TiB <sub>2</sub>	
					12	95.6	α-SiC, TiB <sub>2</sub>	
ST2	60	30	7	3	0	97.4	β-SiC, TiB <sub>2</sub>	YAG, * α-Al <sub>2</sub> O <sub>3</sub>
					2	97.0	β-SiC, TiB <sub>2</sub>	YAG, α-SiC
					6	96.8	α-SiC, TiB <sub>2</sub>	YAG
					12	95.5	α-SiC, TiB <sub>2</sub>	YAG
ST3	50	30	14	6	0	98.1	β-SiC, TiB <sub>2</sub>	YAG, α-Al <sub>2</sub> O <sub>3</sub>
					2	97.2	β-SiC, TiB <sub>2</sub>	YAG, α-SiC
					6	95.9	α-SiC, TiB <sub>2</sub>	YAG
					12	94.7	α-SiC, TiB <sub>2</sub>	YAG

\*Y<sub>3</sub>Al<sub>5</sub>O<sub>12</sub> (yttrium aluminium garnet)

as sintering additives. The Al<sub>2</sub>O<sub>3</sub>–Y<sub>2</sub>O<sub>3</sub> mixtures have been selected because of their effectiveness, compared to other additives, in decreasing the softening temperature and viscosity of secondary phase during liquid-phase-sintering of SiC ceramics.<sup>12,13</sup>

## 2 EXPERIMENTAL PROCEDURE

Commercially available β-SiC (Ibiden Co. Ltd, Japan, Betarundum), TiB<sub>2</sub> (H. C. Starck, Germany, grade F), Al<sub>2</sub>O<sub>3</sub> (Sumitomo Chemicals Co. Ltd, Japan, AKP-30), and Y<sub>2</sub>O<sub>3</sub> powders (H.C. Starck, Germany, fine grade) were used as starting materials. The powder mixtures of SiC–30 wt% TiB<sub>2</sub> containing 5 wt% Al<sub>2</sub>O<sub>3</sub>–Y<sub>2</sub>O<sub>3</sub> (designated as ST1), 10 wt% Al<sub>2</sub>O<sub>3</sub>–Y<sub>2</sub>O<sub>3</sub> (ST2), 20 wt% Al<sub>2</sub>O<sub>3</sub>–Y<sub>2</sub>O<sub>3</sub> (ST3) as sintering additives were ball-milled in ethanol with SiC grinding balls for 24 h. The ratio of Al<sub>2</sub>O<sub>3</sub>:Y<sub>2</sub>O<sub>3</sub> was fixed as 7:3 by weight. Batch compositions are shown in Table 1. The milled slurry was dried, sieved through a 60-mesh screen, and then hot-pressed at 1850°C for 1 h with 20 MPa of applied pressure under Ar. The hot-pressed materials were subsequently annealed at 1950°C for 2, 6, and 12 h under argon to enhance the grain growth of TiB<sub>2</sub> and the β→α phase transformation of SiC.

Densities were measured using the Archimedes method and the relative densities of the specimens were calculated based on the densities of SiC (3.215 g cm<sup>−3</sup>), TiB<sub>2</sub> (4.495 g cm<sup>−3</sup>), Al<sub>2</sub>O<sub>3</sub> (3.987 g cm<sup>−3</sup>), and Y<sub>2</sub>O<sub>3</sub> (5.031 g cm<sup>−3</sup>) assuming the rule of mixtures. Crystalline phases in the sintered specimens were determined by X-ray diffractometry (XRD) using Cu-K<sub>α</sub> radiation. The microstructure was observed by scanning electron microscopy (SEM). Some specimens were polished and plasma etched for observing grain size of SiC. The length and width of SiC grains were determined from the longest and the shortest grain

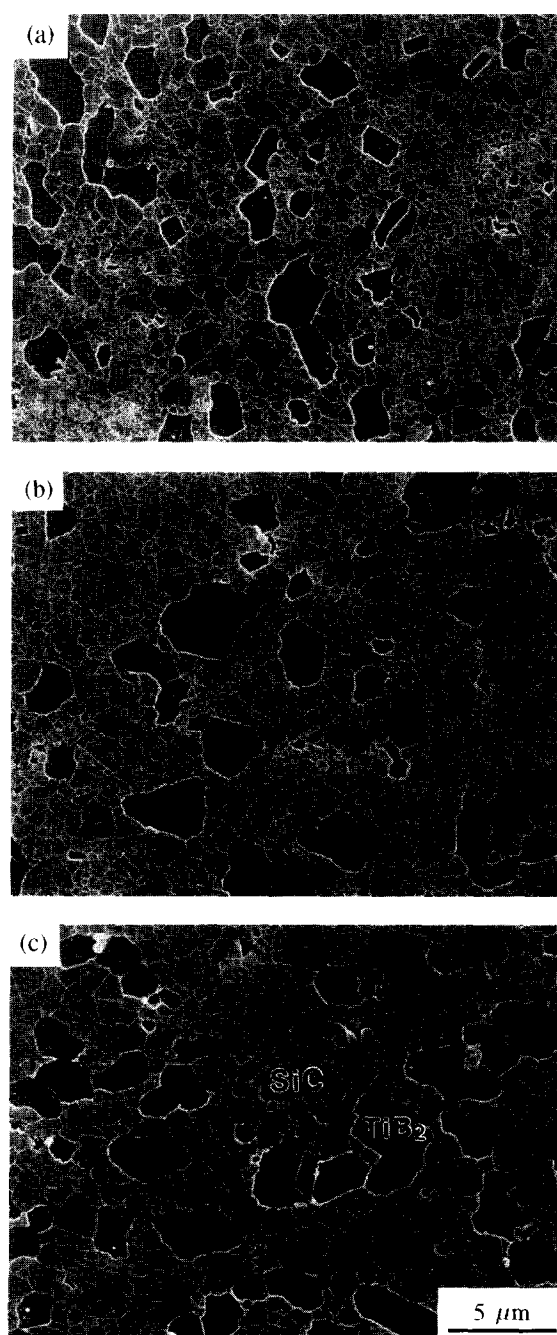


**Fig. 1.** SEM micrographs of hot-pressed SiC–30 wt% TiB<sub>2</sub> composites: (a) 5 wt% Al<sub>2</sub>O<sub>3</sub>–Y<sub>2</sub>O<sub>3</sub>; (b) 10 wt% Al<sub>2</sub>O<sub>3</sub>–Y<sub>2</sub>O<sub>3</sub>; (c) 20 wt% Al<sub>2</sub>O<sub>3</sub>–Y<sub>2</sub>O<sub>3</sub>.

diagonals, respectively, in the two-dimensional image. The grain sizes of SiC in as-hot-pressed composites and TiB<sub>2</sub> were determined from the diameter of circle approximation with equivalent area in the two-dimensional image. A total of 300 to 500 grains per specimens was used for the statistical analysis. The fracture toughness was estimated by measuring crack lengths generated by a Vickers' indenter with a load of 196 N.<sup>14</sup>

### 3 RESULTS AND DISCUSSION

The characteristics of SiC-30 wt% TiB<sub>2</sub> composites are summarised in Table 1. The relative densities of >97% were achieved by hot-pressing with a holding time of 1 h at 1850°C. However, prolonged annealing at 1950°C resulted in a decrease of the relative density, probably due to the formation of volatile components such as AlO, Al<sub>2</sub>O and

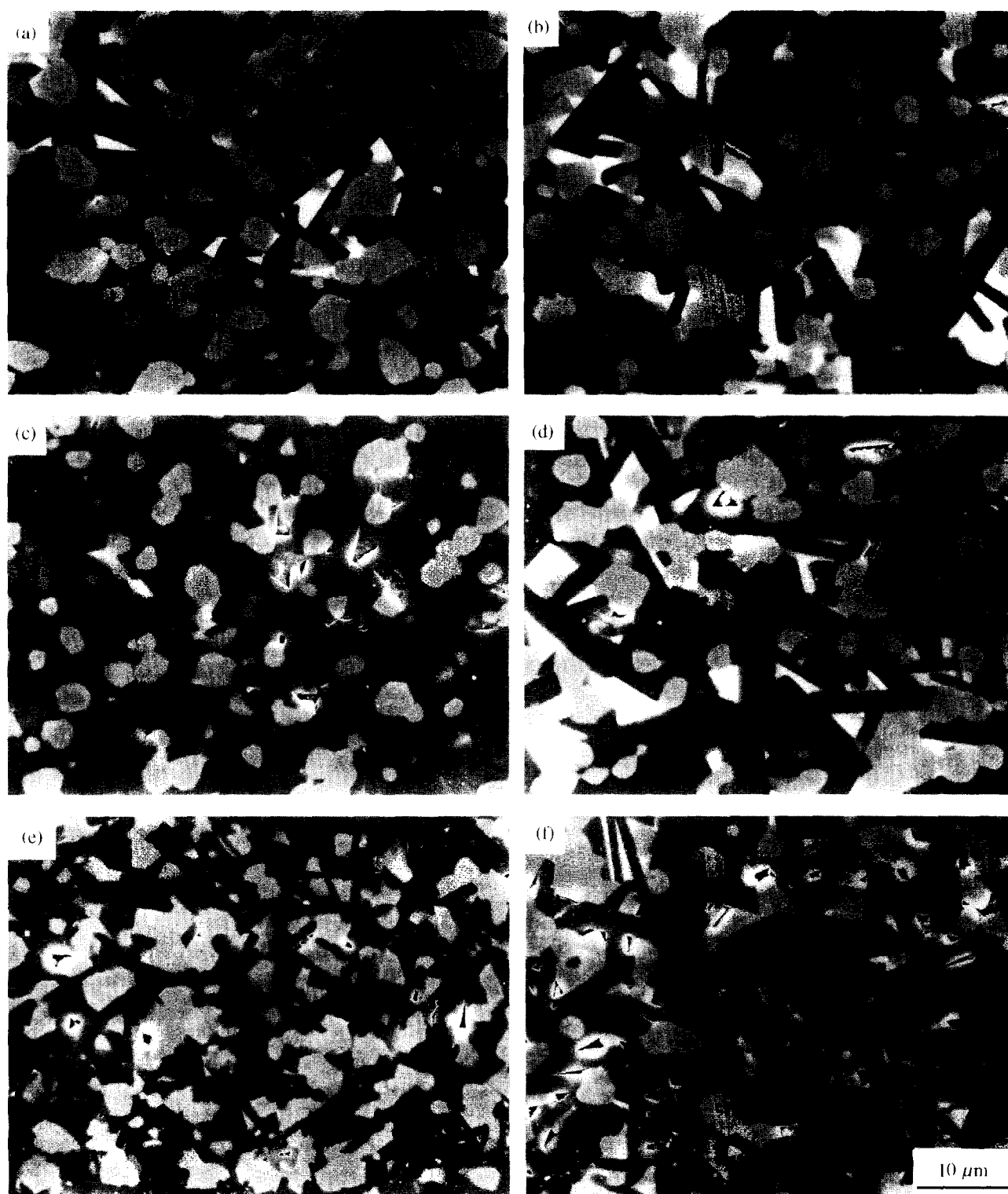


Fig. 2. SEM micrographs of polished cross-sections of annealed SiC-TiB<sub>2</sub> composites: (a) 6-h annealed ST1; (b) 12-h annealed ST1; (c) 6-h annealed ST2; (d) 12-h annealed ST2; (e) 6-h annealed ST3; and (f) 12-h annealed ST3 (refer to Table 1).

Table 2. Microstructural characteristics of hot-pressed and annealed SiC-TiB<sub>2</sub> composites

Materials	Annealing time at 1950°C(h)	SiC grain		
		Aspect ratio	Length×width (μm)	TiB <sub>2</sub> grain size (μm)
ST1	0	—	0.47*	1.40
	2	2.6	2.75×1.04	2.09
	6	3.0	6.37×2.10	2.32
	12	3.1	6.60×2.16	2.38
ST2	0	—	0.58*	1.71
	2	2.7	2.89×1.07	2.16
	6	3.9	7.73×2.00	2.44
	12	4.1	8.49×2.07	2.59
ST3	0	—	0.72*	1.74
	2	3.0	3.25×1.08	2.22
	6	4.6	8.84×1.94	2.51
	12	5.4	11.02×2.03	2.60

\*Average grain size.

CO.<sup>15,16</sup> Higher amounts of additive addition resulted in increase of the sintered density because of the increased amount of liquid phase during hot-pressing and resulted in lower relative density after annealing probably because of the increased volatilization of additives during annealing. Phase analysis of hot pressed ST2 and ST3 materials by XRD showed β-SiC, TiB<sub>2</sub>, YAG and α-Al<sub>2</sub>O<sub>3</sub>. In contrast, phase analysis of hot-pressed ST1 showed β-SiC and TiB<sub>2</sub> only. The 6-h annealed ST2 and ST3 materials were found to be composed of α-SiC, TiB<sub>2</sub> and YAG, indicating the volatilization of α-Al<sub>2</sub>O<sub>3</sub> during annealing. Polymorph of α-SiC was 4H, indicating the occurrence of β→α phase transformation of SiC during annealing.

Figure 1 shows the microstructures of hot-pressed

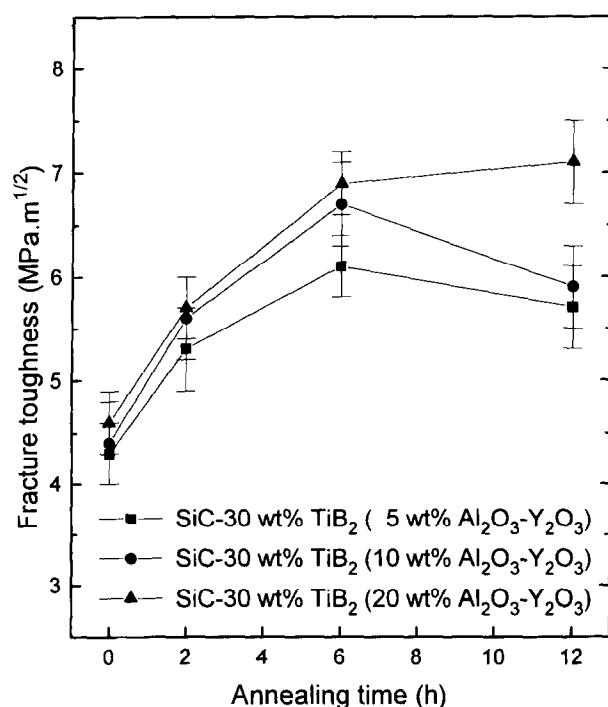


Fig. 3. Relation between fracture toughness and annealing time at 1950°C for ST1, ST2, and ST3 (refer to Table 1).

sed SiC-TiB<sub>2</sub> composites with different amount of additives. As shown, the hot-pressed composites were a two-phase particulate composite consist of randomly distributed TiB<sub>2</sub> grains, whose diameters ranging from 0.5 to 5 μm, and relatively fine, equiaxed SiC matrix grains. The grain size of SiC grains in hot-pressed materials increased from 0.47 μm (ST1) to 0.72 μm (ST3) with increasing the amount of additives, probably due to the increased densification.<sup>15,17</sup>

Figure 2 shows the microstructural change of the composites after annealing at 1950°C for 6 and 12 h, respectively. The bright phase is TiB<sub>2</sub>, the dark grey phase is SiC, and white phase is oxide additives, presumably YAG. The effect of annealing became apparent after 6 h, as indicated by the phase analysis in Table 1, which shows the marked growth of α-SiC. It is well documented that grain growth through the solution-precipitation and the β→α phase transformation of SiC takes place at high temperatures (≥1950°C), especially at the presence of proper liquids.<sup>11,18,19</sup>

The results of image analysis are summarised in Table 2. The average aspect ratio and width of SiC grains increase gradually with annealing time. It indicates that grain growth and β→α phase transformation of SiC take place simultaneously during annealing and the anisotropy in the grain shape of SiC grains increases. As shown in Table 2, the amount of additives also influenced the morphologies of SiC and TiB<sub>2</sub>. The average aspect ratio of SiC grains increased, i.e. from 3.1 for 12-h annealed ST1 to 5.4 for 12-h annealed ST3, with increasing the amount of additives. In contrast, the width of SiC grains decreased slightly, i.e. from 2.2 μm for 12-h annealed ST1 to 2.0 μm for 12-h annealed ST3, with increasing the amount of additives.

SiC grains in ST1 therefore were thicker and shorter than those of ST3 because of the impinge-

ment of grains. It indicates that the anisotropy in the grain shape of SiC grains increases with increasing the amount of additives. Coarsening of TiB<sub>2</sub> grains took place during annealing because of the grain growth of TiB<sub>2</sub> grains. Interestingly, shape of TiB<sub>2</sub> grains changed from equiaxed to matrixlike grains during annealing (Figs 1 and 2). This may be due to the ductile nature of TiB<sub>2</sub> grains yielding to the grain growth of elongated

$\alpha$ -SiC grains and forming a matrixlike microstructure.

Variation of fracture toughness with annealing time is shown in Fig. 3. As shown, the fracture toughnesses of materials increase with annealing time at 1950°C. The fracture toughness of 12-h annealed ST3 (7.1 MPa m<sup>1/2</sup>) was approximately 50% higher than that of as-hot-pressed composites (4.6 MPa m<sup>1/2</sup>). The increased fracture toughness

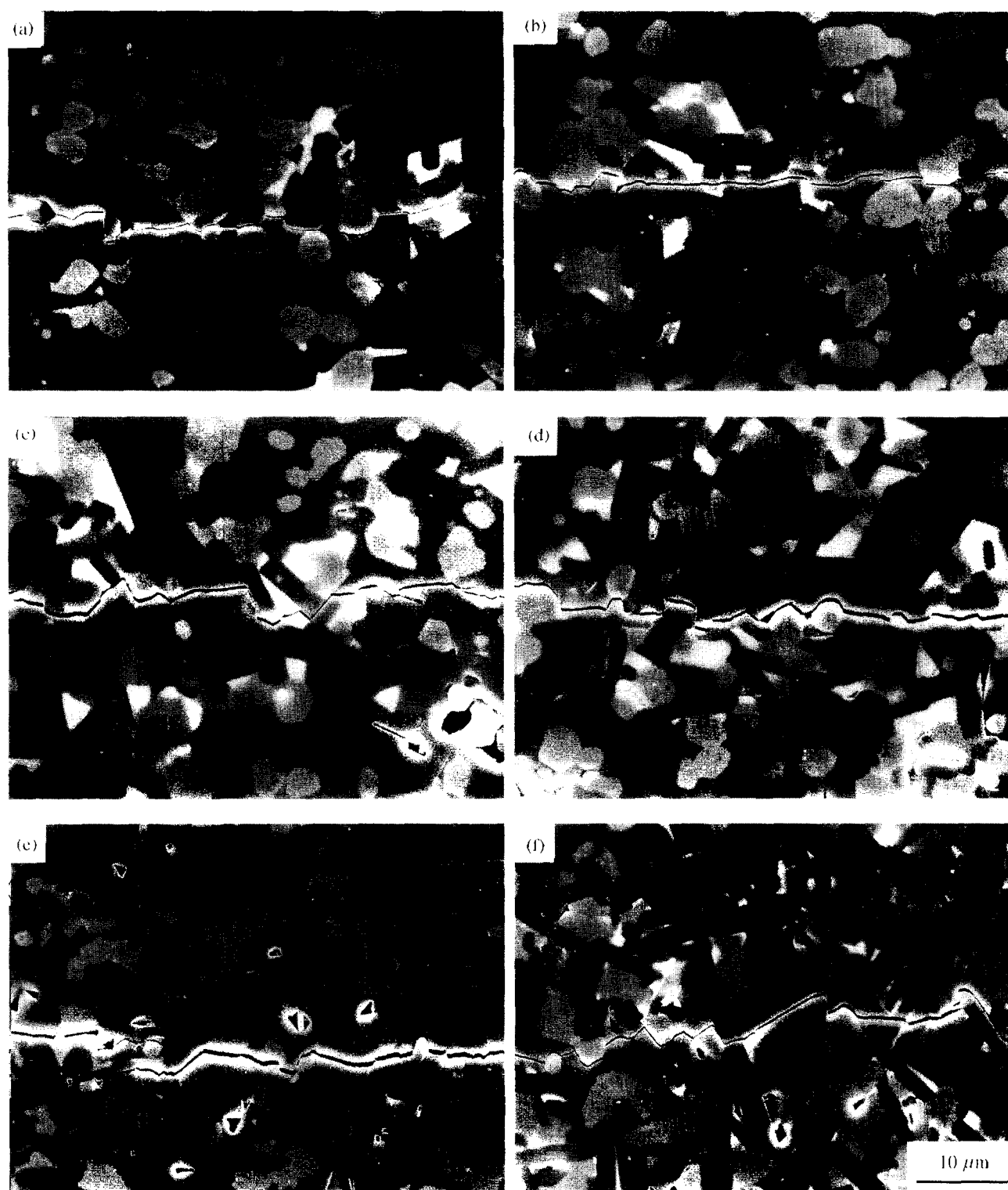


Fig. 4. SEM micrographs of crack paths induced by a Vickers indenter: (a) 6-h annealed ST1; (b) 12-h annealed ST1; (c) 6-h annealed ST2; (d) 12-h annealed ST2; (e) 6-h annealed ST3; and (f) 12-h annealed ST3 (refer to Table I)

may be related to the microstructure. When the annealing time was increased, the shape of SiC grains changed from equiaxed (as-hot-pressed and 2-h annealed materials) to elongated grains (6-h and 12-h annealed materials) and the average aspect ratio and width of SiC grains and the average grain size of TiB<sub>2</sub> grains increased because of grain growth of both SiC and TiB<sub>2</sub> grains. The increase in fracture toughness with annealing time is due to the enhanced bridging and crack deflection by the elongated  $\alpha$ -SiC grains and coarse TiB<sub>2</sub> grains, as observed in Fig. 4. The increase in fracture toughness of non-cubic ceramics with increasing grain size, owing to the enhanced crack definition and bridging, has been reported by several investigators.<sup>20–23</sup>

The effect of the amount of additives on the fracture toughness of the SiC–TiB<sub>2</sub> composites is also shown in Fig. 3. The fracture toughness increased with increasing the amount of additives. When relatively high amount of additives were added (ST3), weak interface boundaries due to thermal expansion mismatch between the second-phase YAG and SiC and/or TiB<sub>2</sub> was maintained after long-time annealing because of the sufficient amount of additives, leading to the enhanced crack bridging and deflection, as observed in Fig. 4(e) and (f). In contrast, when small amount of additives were added (ST1), the second phase-insufficient regions might be introduced due to the evaporation of additives during annealing,<sup>19,24</sup> leading to the increased tendency of transgranular fracture, as observed in Fig. 4(a) and (b). Therefore, the decrease in fracture toughness of 12-h annealed ST1 and ST2, although the length and width of  $\alpha$ -SiC grains were increased compared with those of 6 h annealed ST1 and ST2, was attributed to the increasing tendency of transgranular fracture and pore formation with prolonged annealing, as shown in Fig. 4(b) and (d). This phenomenon is quite similar to the one observed in in-situ-toughened SiC–TiC<sub>2</sub> composites.<sup>25</sup> Present results suggest that further increase in fracture toughness of in-situ-toughened SiC–TiB<sub>2</sub> composites may be possible by controlling the length and width of the elongated  $\alpha$ -SiC grains and adding the optimum amount of additives.

#### 4 SUMMARY

In-situ-toughened SiC–30 wt% TiB<sub>2</sub> composites were fabricated from  $\beta$ -SiC and TiB<sub>2</sub> powders with Al<sub>2</sub>O<sub>3</sub>–Y<sub>2</sub>O<sub>3</sub> additives by hot-pressing and subsequent annealing. The introduction of larger-amount of additives, within the amount range studied (5–20 wt%), accelerated the grain growth

of elongated  $\alpha$ -SiC grains with higher aspect ratio and maintained the weak interface boundaries after long-time annealing, resulting in the improved fracture toughness. The fracture toughness of 12-h annealed materials with 20 wt% additives was as high as 7.1 MPa m<sup>1/2</sup>, owing to bridging and crack deflection by the elongated  $\alpha$ -SiC grains and coarse TiB<sub>2</sub> grains, approximately 20% higher than that of 12-h annealed materials with 5 wt% additives (5.7 MPa m<sup>1/2</sup>).

#### REFERENCES

1. JANNEY, M. A., Mechanical properties and oxidation behavior of a hot-pressed SiC–15 vol% TiB<sub>2</sub> composites. *Am. Ceram. Soc. Bull.*, **66**(2) (1987) 322–324.
2. KIM, Y. W., CHOI, H. J., LEE, J. G., LEE, S. W. & CHUNG, S. K., Properties of electrical discharge machinable SiC–TiB<sub>2</sub> composites. *Kor. J. Ceram.*, **1**(3) (1995) 125–130.
3. OHYA, Y., HOFFMANN, M. J. & PETZOW, G., Sintering of in-situ synthesized SiC–TiB<sub>2</sub> composites with-improved fracture toughness. *J. Am. Ceram. Soc.*, **75**(9) (1992) 2479–2483.
4. KIM, Y. W. & LEE, J. G., Effect of polycarbosilane addition on mechanical properties of hot-pressed silicon carbide. *J. Mater. Sci.*, **27** (1992) 4746–4750.
5. KRISTIC, V. D., Optimization of mechanical properties in SiC by control of the microstructure. *Mater. Res. Soc. Bull.*, **20**(2) (1995) 46–48.
6. CHOI, H. J., KIM, Y. W. & LEE, J. G., Effect of amount and composition of additives on the fracture toughness of silicon nitride. *J. Mater. Sci. Lett.*, **15** (1996) 375–377.
7. McMURTRY, C. H., BOECKER, W. D. G., SESHADRI, S. G., ZANGHI, J. S. & GARNIER, J. E., Microstructure and material properties of SiC–TiB<sub>2</sub> particulate composites. *Am. Ceram. Soc. Bull.*, **66**(2) (1987) 325–329.
8. TANI, T. & WADA, S., SiC matrix composites reinforced with internally synthesized TiB<sub>2</sub>. *J. Mater. Sci.*, **25** (1990) 157–160.
9. CHO, K. S., KIM, Y. W., CHOI, H. J. & LEE, J. G., SiC–TiC and SiC–TiB<sub>2</sub> composites densified by liquid-phase sintering. *J. Mater. Sci.*, **31** (1996) 6223–6228.
10. CHO, K. S., CHOI, H. J., LEE, J. G. & KIM, Y. W., In-situ enhancement of toughness of SiC–TiB<sub>2</sub> composites. *J. Mater. Sci.*, **33** (1998) 211–214.
11. PADTURE, N. P., In situ-toughened silicon carbide. *J. Am. Ceram. Soc.*, **77**(2) (1994) 519–523.
12. MULLA, M. A. & KRISTIC, V. D., Low-temperature pressureless sintering of  $\beta$ -silicon carbide with aluminium oxide and yttrium oxide additions. *Am. Ceram. Soc. Bull.*, **70**(3) (1991) 439–443.
13. KIM, Y. W., CHO, K. S. & LEE, J. G., Effect of large  $\alpha$ -silicon carbide seed grains on microstructure and fracture toughness of pressureless-sintered  $\alpha$ -silicon carbide. *Kor. J. Ceram.*, **2**(1) (1996) 39–42.
14. ANSTIS, G. R., CHANTIKUL, P., LAWN, B. R. & MARSHALL, D. B., A critical evaluation of indentation techniques for measuring fracture toughness: I, direct crack measurements. *J. Am. Ceram. Soc.*, **64**(9) (1981) 533–538.
15. KIM, Y. W., TANAKA, H., MITOMO, M. & OTANI, S., Influence of powder characteristics on liquid phase sintering of silicon carbide. *J. Ceram. Soc. Jpn*, **103**(3) (1995) 257–261.

16. MULLA, M. A. & KRISTIC, V. D., Pressureless sintering of  $\beta$ -SiC with Al<sub>2</sub>O<sub>3</sub> additions. *J. Mater. Sci.*, **29** (1994) 934–938.
17. GERMAN, R. M., *Sintering Theory and Practice*. John Wiley & Sons, Inc., New York, 1996, pp. 293–299.
18. SIGL, L. S. & KLEEBE, H. J., Core/rim structure of liquid-phase-sintered silicon carbide. *J. Am. Ceram. Soc.*, **76**(3) (1993) 773–776.
19. LEE, S. K. & KIM, C. H., Effects of  $\alpha$ -SiC versus  $\beta$ -SiC starting powders on microstructure and fracture toughness of SiC sintered with Al<sub>2</sub>O<sub>3</sub>-Y<sub>2</sub>O<sub>3</sub> additions. *J. Am. Ceram. Soc.*, **77**(6) (1994) 1655–1658.
20. RICE, R. W., FREIMAN, S. W. & BECHER, P. F., Grain-size dependence of fracture energy in ceramics: I. Experimental. *J. Am. Ceram. Soc.*, **64**(6) (1981) 345–350.
21. RICE, R. W., FREIMAN, S. W. & BECHER, P. F., Grain-size dependence of fracture energy in ceramics: II, A model for noncubic materials. *J. Am. Ceram. Soc.*, **64**(6) (1981) 350–354.
22. SWANSON, P. L., FAIRBANKS, C. J., LAWN, B. R., MAI, Y. W. & HOCKEY, B. J., Crack-interface grain bridging as a fracture resistance mechanism in ceramics: I, Experimental study on alumina. *J. Am. Ceram. Soc.*, **70**(4) (1987) 279–289.
23. RODEL, J., Interaction between crack definition and crack bridging. *J. Eur. Ceram. Soc.*, **10** (1992) 143–150.
24. KLEEBE, H. J., SiC and Si<sub>3</sub>N<sub>4</sub> materials with improved fracture resistance. *J. Eur. Ceram. Soc.*, **10** (1992) 151–159.
25. CHO, K. S., KIM, Y. W., CHOI, H. J. & LEE, J. G., *In-situ*-toughened silicon carbide-titanium carbide composites. *J. Am. Ceram. Soc.*, **79**(6) (1996) 1711–1713.